



室蘭工業大学

学術資源アーカイブ

Muroran Institute of Technology Academic Resources Archive



Design of polarization splitter and rotator using function-expansion based topology optimization considering two-layer structure

メタデータ	言語: eng 出版者: 日本シミュレーション学会 公開日: 2019-07-09 キーワード (Ja): キーワード (En): Topology optimization, Function expansion method, Polarization splitter and rotator 作成者: 富岡, 瞬, 田中, 智大, 森, 洸遥, 辻, 寧英 メールアドレス: 所属:
URL	http://hdl.handle.net/10258/00009949

Design of polarization splitter and rotator using function-expansion based topology optimization considering two-layer structure

Shun Tomioka¹, Tomohiro Tanaka¹, Koyo Mori¹, Yasuhide Tsuji^{1,*}

¹Muroran Institute of Technology, Division of Information and Electronic Engineering

*y-tsuji@mmm.muroran-it.ac.jp

Received: October 29, 2018; Accepted: February 12, 2019; Published: March 15, 2019

Abstract. Function expansion based topology optimization method for optical waveguide devices has been proposed as an automatic design method which can produce an optimal device structure having an arbitrary topology. In this paper, we aim to extend the function expansion based topology optimization method to the design problems of three-dimensional photonic devices with structural variation in the depth direction. We confirm the effectiveness of our approach through the design example of the polarization splitter and rotator which utilizes structural asymmetry in the depth direction.

Keywords: Topology optimization, function expansion method, polarization splitter and rotator

1. Introduction

Due to the spread of the Internet and smartphones, communication traffic has been increasing, and high speed and large capacity optical communication systems are required. In order to respond to such demands, it is indispensable to develop higher performance photonic devices, and the related researches are actively conducted. Recently, topology optimization methods have begun to be used to realize high-performance optical waveguide devices [1–4]. The topology optimal design method of photonic devices using function expansion method for structural representation has been also proposed [5, 6]. The function expansion method has advantages such as allowing a design with a high degree of freedom using a small number of design variables. However, in the past study about function expansion method, only a two-dimensional geometry is designed, even in the case of a three-dimensional photonic devices [6]. In this paper, in order to enable structural variation along the depth direction, we aim to design three-dimensional photonic devices having a layered structure by using a function expansion method. In this approach, each layer is able to be designed independently of each other. We confirm the effectiveness of the proposed approach through a design of

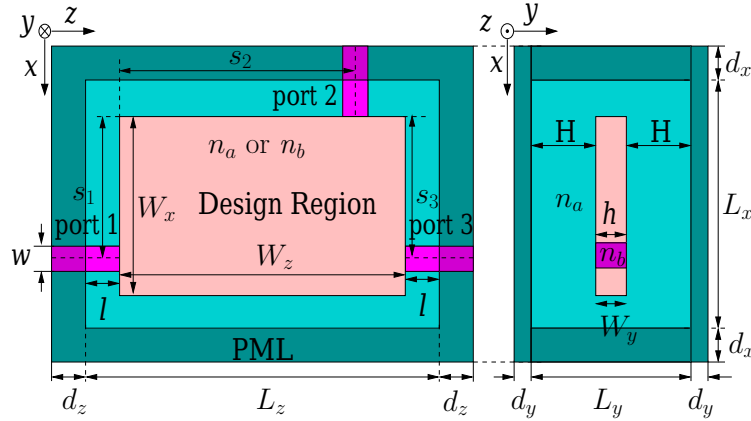


Figure 1: Design model of PSR.

polarization splitter and rotator (PSR) [7]. PSR is one of the key devices in recent photonic circuits and is used in polarization diversity, polarization multiplexing, and so on. In order to realize polarization conversion, structural asymmetry along the depth direction has to be required and layered structure considered here is thought to be effective.

2. Topology optimization method for photonic devices with layered structure

2.1. Representation of refractive index distribution for two-layer structure with function-expansion method

We consider a design problem of PSR whose design region consists of two materials with different refractive indices of n_a and n_b as shown in Fig. 1. In order to express a layered structure, we extend the function expansion method [5] and express the refractive index distribution as follows:

$$n^2(x, y, z) = n_a^2 + (n_b^2 - n_a^2)H(w_i(x, z)) \quad (1)$$

$$w_i(x, z) = \sum_{j=1}^N c_j^{(i)} f_j(x, z) \quad (i = 1, 2) \quad (2)$$

where the function $H(w_i)$ is used to binarize a continuous value of $w_i(x, z)$ into either n_a or n_b . The function $w_i(x, z)$ which determines the geometry of the i -th layer is independently optimized in each layer. In this expression, the device structure is determined by the amplitude coefficient $c_j^{(i)}$ of each basis function and those are the design parameters in the optimal design.

2.2. Full-vectorial finite element method

In order to analyze three-dimensional photonic devices, we employ the full-vectorial finite element method (FV-FEM). The basic equation to express the light propagating behavior in photonic devices is given as follows:

$$\nabla \times (p \nabla \times \Phi) - k_0^2 q \Phi = \mathbf{0} \quad (3)$$

where k_0 is a free-space wavenumber, and p , q , and Φ are defined as follows:

$$\begin{cases} p = 1 & q = n^2 & \text{for } \Phi = \mathbf{E} \\ p = 1/n^2 & q = 1 & \text{for } \Phi = \mathbf{H} \end{cases} \quad (4)$$

where n is a refractive index distribution. Applying FV-FEM with tetrahedral edge element to (3), the following simultaneous linear equation is obtained [6]:

$$[P]\{\Phi\} = \{u\} \quad (5)$$

where $[P]$ is a FEM matrix and $\{u\}$ is a vector related to an incidence condition. Once the propagating field $\{\Phi\}$ is obtained, the scattering parameter into port n is calculated as follows:

$$S_{n1} = \{g_n\}^T \{\Phi\} \quad (6)$$

where $\{g_n\}$ is the vector related to the modal field in port n .

2.3. Sensitivity analysis based on adjoint variable method

In order to optimize design parameters, we have to evaluate a sensitivity of a device performance with respect to each design parameter. To efficiently evaluate the sensitivity, we employ the adjoint variable method and optimize the design parameters by using the gradient descent method. The sensitivity of the scattering parameter S_{n1} is expressed as follows [6]:

$$\frac{\partial S_{n1}}{\partial c_j^{(i)}} = -\{\lambda_n\}^T \frac{\partial [P]}{\partial c_j^{(i)}} \{\Phi\} \quad (7)$$

where the adjoint variable $\{\lambda_n\}$ is calculated by

$$[P]^T \{\lambda_n\} = \{g_n\}. \quad (8)$$

2.4. Structural smoothing filter

In the topology optimization, due to the high degree of freedom of the structure, a complicated structure which is difficult to be actually fabricated may happen to be obtained. In order to avoid such an unrealistic device structure, we consider the simplification of the structure using the Gaussian filter [8].

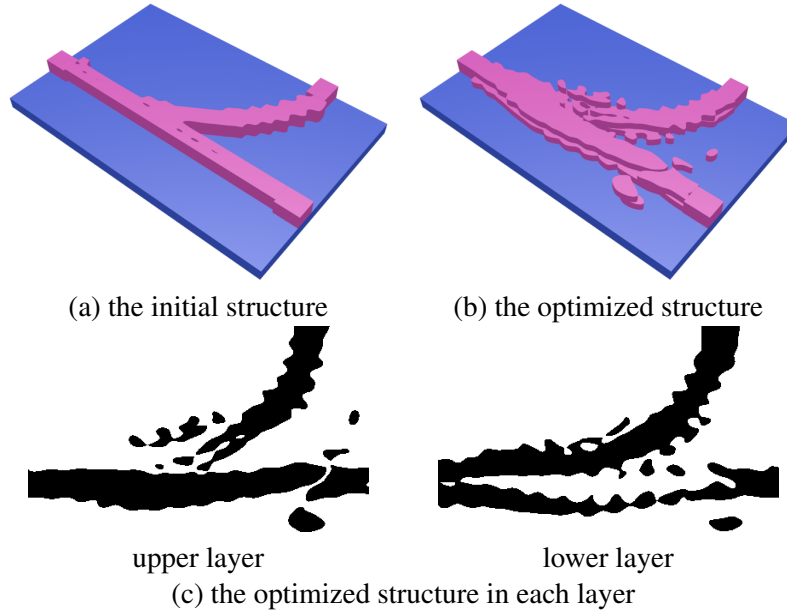


Figure 2: Topology optimized PSR with two layers.

When the wavenumber spectrum of the structural function $w(x, z)$ is given by $W(k_x, k_z)$, the spectrum of the smoothed structure, $W'(k_x, k_z)$, is determined by

$$W'(k_x, k_z) = W(k_x, k_z)G(k_x, k_z). \quad (9)$$

Here, $G(k_x, k_z)$ is the filter function in the wavenumber domain and is defined as follows:

$$G(k_x, k_z) = \frac{1}{2\pi\sigma^2} \exp\left(-\frac{k_x^2 + k_z^2}{2\sigma^2}\right). \quad (10)$$

In the wavenumber domain, the components with higher wavenumber is suppressed by this filter. Here, the smaller the σ is, the simpler structure is obtained, however, the device performance may be degraded. Thus, the value of σ should be appropriately selected.

3. Optimization of polarization splitter and rotator

3.1. Design without smoothing filter

We consider the design model as shown in Fig. 1. The structural parameters are assumed to be $w = 0.4 \mu\text{m}$, $h = 0.3 \mu\text{m}$, $l = 0.5 \mu\text{m}$, $W_x = 3 \mu\text{m}$, $W_y = 0.3 \mu\text{m}$, $W_z = 5 \mu\text{m}$, $s_1 = s_3 = 2.3 \mu\text{m}$, $s_2 = 4.2 \mu\text{m}$, $L_x = 4 \mu\text{m}$, $L_y = 1.3 \mu\text{m}$, $L_z = 6 \mu\text{m}$, $H = 0.5 \mu\text{m}$, $d_x = d_z = 0.5 \mu\text{m}$, and $d_y = 0.2 \mu\text{m}$. The refractive indices of the materials are assumed to be $n_a = 1.45$ and $n_b = 3.4$, respectively. We design a PSR which can split E_{11}^x and E_{11}^y modes launched from port 1 into port 2 and port 3, respectively, and convert E_{11}^y mode into

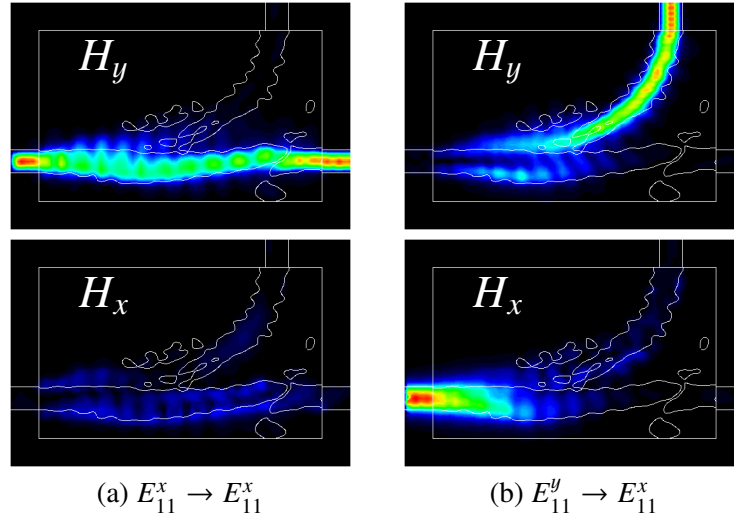


Figure 3: Propagating field in the optimized PSR.

E_{11}^x mode. The objective function to be minimized is given as follows:

$$\text{Minimize } C = \begin{cases} \left(1 - |S_{31}^{E_{11}^x \rightarrow E_{11}^x}|^2\right)^2 & (E_{11}^x \text{ incidence}) \\ \left(1 - |S_{21}^{E_{11}^y \rightarrow E_{11}^x}|^2\right)^2 & (E_{11}^y \text{ incidence}) \end{cases} \quad (11)$$

where S_{31} and S_{21} are the scattering parameters from port 1 to port 3 and port 2, respectively. First, we design the PSR without using structural smoothing filter. The structure expressing function $w_i(x, z)$ is assumed to be Fourier series [5] and the number of design parameters is set as 32×32 in each layer. Figure 2 shows the initial structure for this optimization and the obtained optimized structure. Figure 3 shows the propagating field in the optimized PSR. The normalized output powers are $0.933(E^x \rightarrow E^x)$ in port 3 and $0.957(E^y \rightarrow E^x)$ in port 2, respectively, thus the desired operation of PSR is realized. However, we can see that the optimized device has a little bit complicated and fine structure.

3.2. Design with smoothing filter

We consider the same design problem of PSR as that in the previous subsection and aim to obtain simpler optimized structure by using the structural smoothing filter. In the following optimization, the filtering process is added at each iteration step of the optimization. First, in order to investigate the filter effect and estimate an appropriate value of σ , we design a PSR by using the Gaussian filter with different filter width. The same initial structure as that in the previous subsection is employed in this discussion. Figure 4 shows the normalized output power in the optimized PSR as a function of the value of σ and Fig. 5 shows the optimized structure for each σ . From these results, it is observed that the output power decreases as the structure is simplified as expected. In order to get the sufficient simplification effect, σ is set to be 100 in the following design example.

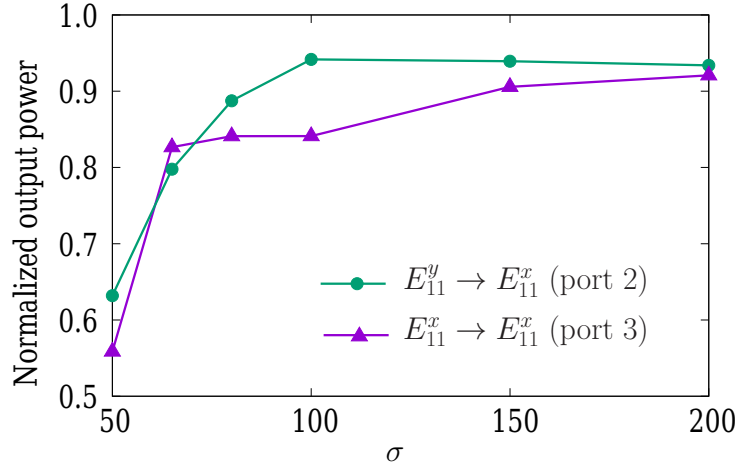


Figure 4: Normalized output power in the optimized structure as a function of σ .

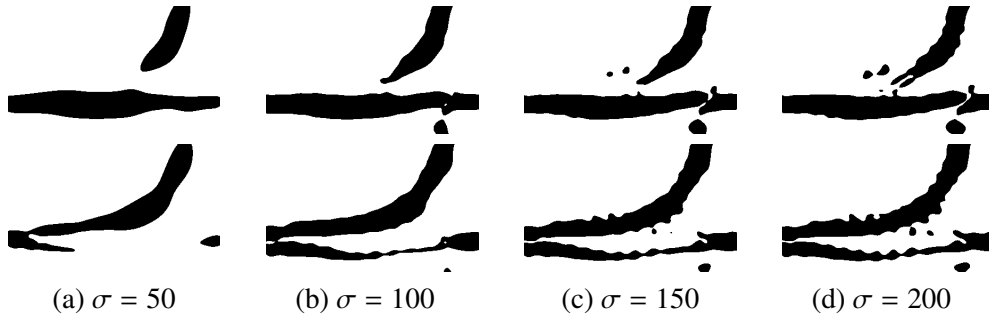


Figure 5: Differences in smoothed structures depending on the value of σ .

Finally, we design the PSR by using the optimized structure in Fig. 2(b) as an initial structure and compare the device performance between the structure in Fig. 2(b) and the smoothed optimized structure. Figure 6 shows the optimized structure by using the smoothing filter with σ of 100. The propagating field in this PSR is shown in Fig. 7. It is seen that the device structure is greatly simplified compared with the optimized structure obtained in the previous subsection. The normalized output powers are 0.865($E^x \rightarrow E^x$) in port 3 and 0.857($E^y \rightarrow E^x$) in port 2, respectively. Figure 8 shows a wavelength dependence of the transmission power of the optimized PSRs with and without using smoothing filter. Since the optimization is performed at a wavelength of $1.55 \mu\text{m}$, in the structure optimized without a smoothing filter, the higher transmittance is obtained at this wavelength. However, the smoothed structure can be used over the wide wavelength range compared with the unsmoothed structure. These results show that the structural smoothing is effective to not only make fabrication easier but also make operation band wider.

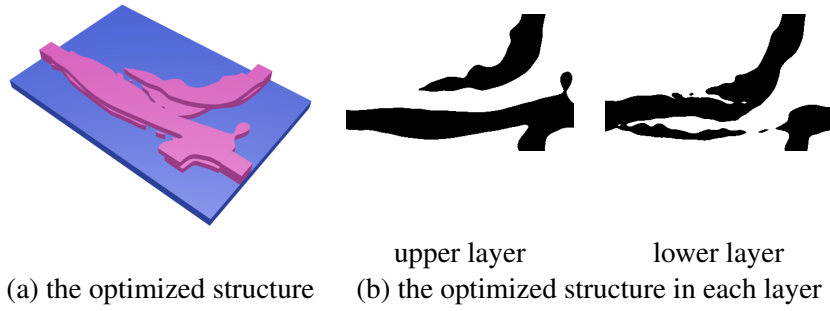


Figure 6: The optimized PSR designed by using the smoothing filter($\sigma = 100$).

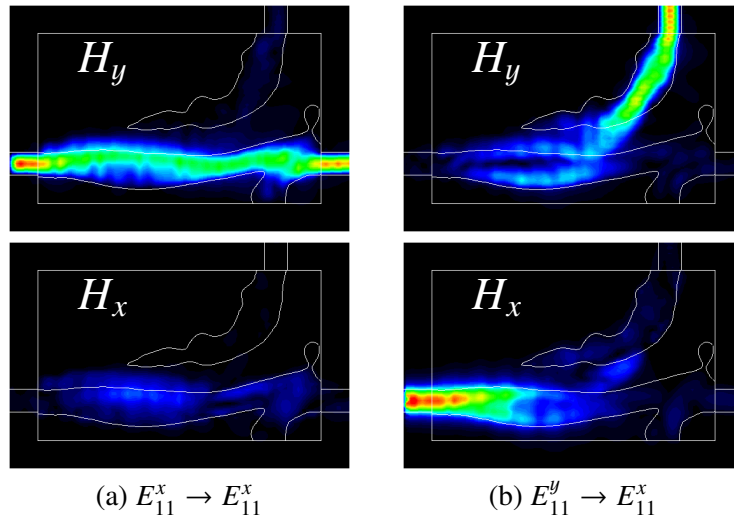


Figure 7: Propagating field in the optimized PSR designed by using the smoothing filter($\sigma = 100$).

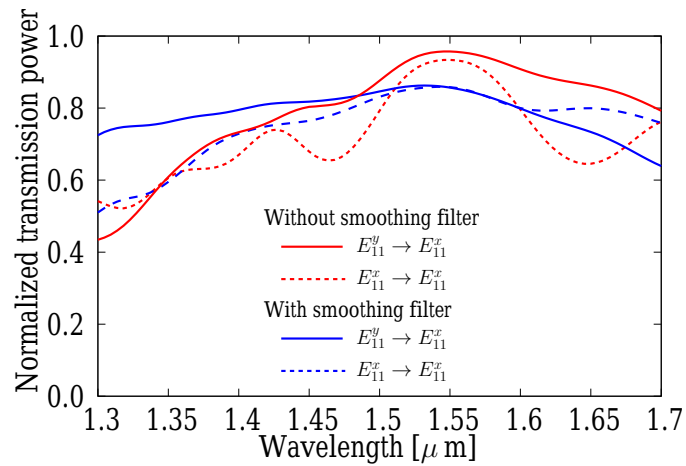


Figure 8: Wavelength dependence of the smoothed structure(Fig. 6) and unsmoothed structure(Fig. 2).

4. Conclusion

We extended the function expansion based topology optimization method to design two-layer structure. The validity of our approach was confirmed through the design example of a PSR. Furthermore, considering the actual fabrication of a PSR, we investigated the structural smoothing filter to obtain a simplified optimized structure. We showed a possibility to obtain a simplified structure by using a Gaussian filter that suppresses higher frequency components in the Fourier series.

References

- [1] L. H. Frandsen, Y. Elesin, L. F. Frellsen, M. Mitrovic, Y. Ding, O. Sigmund, and K. Yvind: Topology optimized mode conversion in a photonic crystal waveguide fabricated in silicon-on-insulator material, *Opt. Express*, 22:7 (2014), 8525–8532.
- [2] M B. Dhring and O Sigmund: Optimization of extraordinary optical absorption in plasmonic and dielectric structures, *J. Opt. Soc. Amer. B.*, 30:5 (2013), 1154–1160.
- [3] Z. Yu, H. Cui, and X. Sun: Genetic-algorithm-optimized wideband on-chip polarization rotator with an ultrasmall footprint *Opt. Lett.*, 42:16 (2017), 3093–3096.
- [4] J. Huang, J. Yang, D. Chen, X. He, Y. Han, J. Zhang, and Z. Zhang: Ultra-compact broadband polarization beam splitter with strong expansibility, *Photon. Res.*, 6:6 (2018), 574–578.
- [5] Y. Tsuji, and K. Hirayama: Design of optical circuit devices using topology optimization method with function-expansion-based refractive index distribution, *IEEE Photon. Technol. Lett.*, 20:12 (2008), 982–984.
- [6] T. Yasui, Y. Tsuji, J. Sugisaka, and K. Hirayama: Design of three-dimensional optical circuit devices by using topology optimization method with function-expansion-based refractive index distribution, *J. Lightw. Technol.*, 31:23 (2013), 3765–3770.
- [7] L. M. Augustin, R. Hanfoug, J. J. G. M. van der Tol, W. J. M. de Laat, M. K. Smit: A Compact Integrated Polarization Splitter/Converter in InGaAsPInP, *IEEE Photon. Technol. Lett.*, 19:17 (2007), 1286–1288.
- [8] H. Goto, Y. Tsuji, T. Yasui, and K. Hirayama: A study on optimization of waveguide dispersion property using function expansion based topology optimization method, *IEICE Trans. Electron.*, E97-C:7 (2014), 670–676.